AIAA 79-1727R

A New Look at Classical vs Modern Homing Missile Guidance

F. William Nesline* and Paul Zarchan†
Raytheon Company, Bedford, Mass.

Modern guidance systems are generally accepted to yield better performance than classical proportional navigation systems. However, it is not always recognized that this better performance carries with it certain costs in improved components or additional instruments. This paper compares a modern guidance system (MGS) to a classical proportional navigational (PN) homing missile guidance system in terms of performance, robustness, and ease of implementation. Quantitative first-order miss distances are compared to show that MGS has the smallest miss if component tolerances can be met, but as component tolerances or measurement errors degrade, MGS degrades faster than PN until, at relatively large component or measurement errors, PN has less miss distance than MGS.

Nomenclature

e = error in estimate, ft
HE = heading error, rad
n_c = missile acceleration, ft/s^2
N' = effective navigation ratio
t_F = time of flight, s
U_n = white noise with power spectral density Φ_N
U_s = white noise with power spectral density Φ_s
V_c = closing velocity, ft/s
V_M = missile velocity, ft/s
V_T = target velocity, ft/s
Y = relative missile-target separation, ft
Y_T = target position, ft
Y_T^* = measured target position, ft
$\dot{Y}_T$ = target rate, ft/s
$\ddot{Y}_T$ = target acceleration, ft/s^2
$\hat{Y}_T$ = estimated target position, ft
λ = line-of-sight angle, rad
$\dot{\lambda}$ = line-of-sight rate, rad/s

Introduction

DURING the 1960's modern control theory was used in theoretical studies of closed form guidance laws for interceptor missiles. It was shown that proportional navigation (PN) was an optimal solution to the linear guidance problem in the sense of producing zero miss distance for the least integral square control effort with a zero lag guidance system in the absence of target maneuver.[1] This important result gave credibility to the use of modern control theory as a tool that many analysts have used to derive missile guidance laws.[2-4] Although much has been written concerning the mathematics of guidance, little, if any, has appeared in the open literature concerning the practical implementation of a modern guidance system (MGS).

Proportional navigation has been in use for over three decades on radar, television, and infrared homing missile systems because of its effectiveness.[5,6] Although PN was apparently known by the German scientists at Pennemünde, no application using PN was reported.[7] It was first studied by Yuan and others during World War II at the RCA Laboratories under the auspices of the U.S. Navy[8]; it was extensively studied by Bennett and Matthews at Hughes Aircraft and implemented in a pulse radar system[9]; and it was fully developed by Rosen and Fossier for a continuous-wave radar system at Raytheon Company. The latter development included a closing velocity multiplier to compensate the guidance law dynamically in flight for changing engagement geometry. After World War II, the U.S. work on PN was declassified and first appeared in the *Journal of Applied Physics*.[10]

The purpose of this paper is to compare both classical and modern methods of guidance in terms of performance and implementation. Both guidance philosophies are reviewed and typical implementations are discussed. Finally both methods of guidance are compared in terms of performance and sensitivity to errors in implementation.

Proportional Navigation

Proportional navigation is a method of guidance in which the missile acceleration is made proportional to the line-of-sight rate. The geometry of an idealized intercept in which the missile and target are closing on each other at constant speed is shown in Fig. 1. Here movement of the missile and target cause the line of sight to rotate through a small angle λ, indicating a differential displacement y between target and missile perpendicular to the reference. The PN guidance law is an attempt to mechanize an acceleration command n_c perpendicular to the line of sight according to

$$n_c = N' V_c \dot{\lambda} \tag{1}$$

where N' is the effective navigation ratio, V_c is the closing velocity, and $\dot{\lambda}$ is the line-of-sight rate.

The effective navigation ratio determines both the trajectory and acceleration history of the missile. For a zero lag guidance system, PN will result in zero miss distance [$y(t_F)=0$] due to heading error or target maneuver for any N' (assuming infinite missile acceleration capability). This phenomenon is demonstrated clearly for the head-on case in the normalized trajectories shown in Fig. 2. Although relative target-missile displacement during the flight increases with decreasing N', all flights result in zero miss distance. The effective navigation ratio influences the accelerations needed to produce zero miss distance. Normalized missile acceleration histories due to both disturbances are shown in Fig. 3. Here missile acceleration is monotonically decreasing (except for $N'=2$) for a heading error disturbance and

Presented as Paper 79-1727 at the AIAA Guidance and Control Conference, Boulder, Colo., Aug. 6-8, 1979; submitted Nov. 5, 1979; revision received June 6, 1980.

*Consulting Scientist, AMRAAM Guidance and Control, Missile Systems Division. Member AIAA.

†Senior Engineer, System Design Laboratory, Missile Systems Division. Member AIAA.

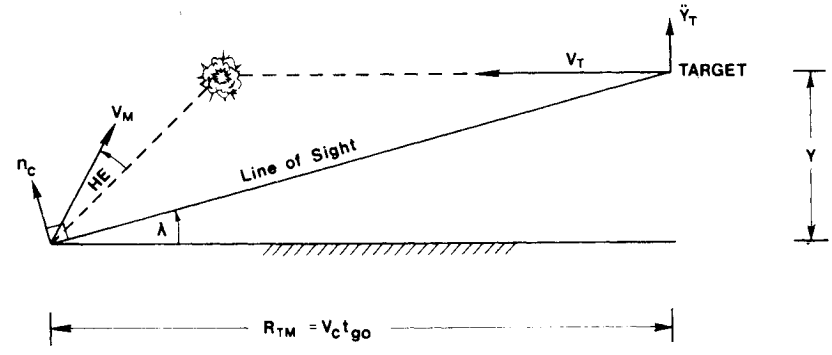

Fig. 1 Intercept geometry.

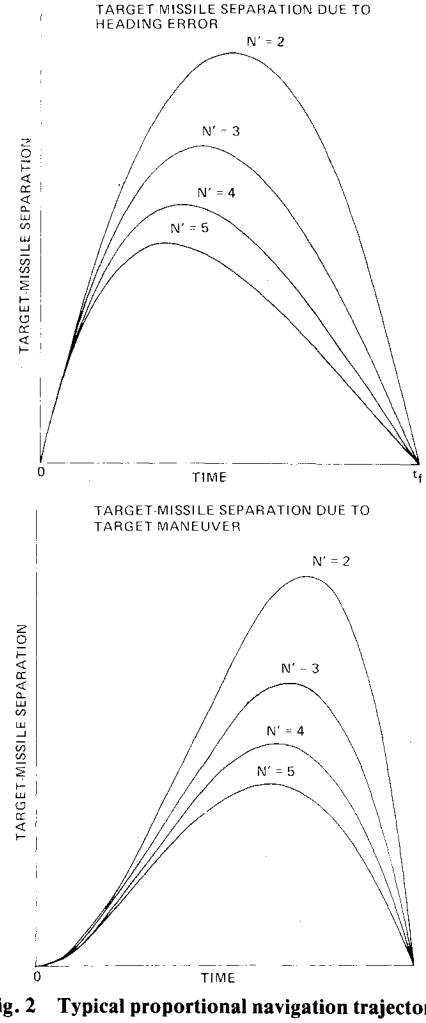

Fig. 2 Typical proportional navigation trajectories.

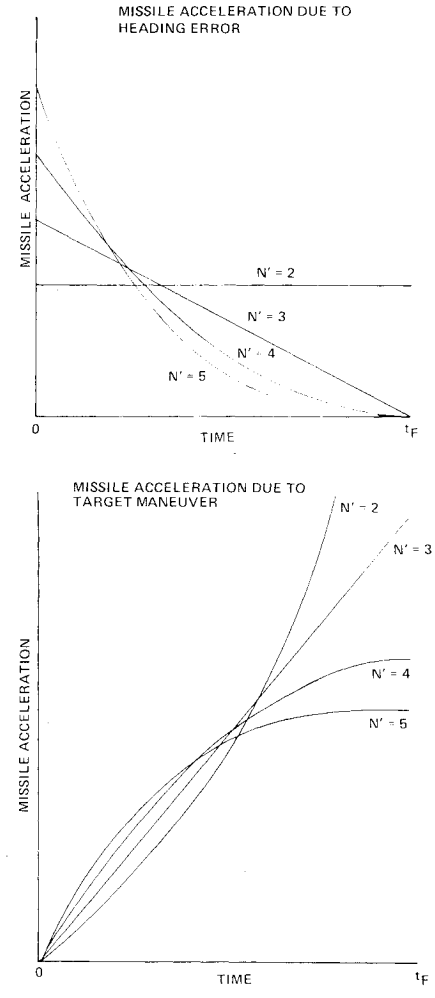

Fig. 3 Typical proportional navigation acceleration histories.

monotonically increasing for a target maneuver disturbance. Figure 3 also shows that increasing N' minimizes the maximum acceleration due to target maneuver but maximizes the maximum acceleration due to heading error. In practice the navigation ratio is held fixed with acceptable values $(3<N'<5)$ determined by noise, radome, and target maneuver considerations.

A typical implementation of a PN guidance system is shown in Fig. 4 where an inertially stabilized seeker is used to measure the boresight error ϵ. This signal, which is proportional to the line-of-sight rate, is low-pass filtered to obtain an estimate of the line-of-sight rate. The time constant T_N of the noise filter can be fixed, as in this implementation, or time varying to account for the range dependence of the measurement noise. The closing velocity can either be estimated, as in infrared applications, or measured by a doppler radar, as in radar homing applications. The resulting acceleration command which is proportional to the line-of-sight rate estimate is applied to an acceleration autopilot that moves wing or tail control surfaces so as to develop the commanded acceleration.

Augmented Proportional Navigation

Other guidance concepts such as those used in modern guidance systems can best be understood by studying proportional navigation. It can be observed from Fig. 1 that PN is mathematically equivalent to

$$n_c = N' V_c \dot{\lambda} = N' V_c \frac{\mathrm{d}}{\mathrm{d}t}\left(\frac{y}{V_c t_{go}}\right) = \frac{N'}{t_{go}^2}\left[y + \dot{y} t_{go}\right] \qquad (2)$$

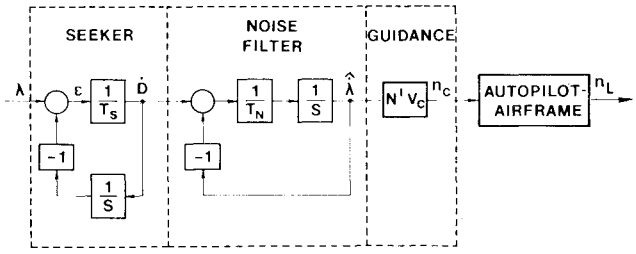

Fig. 4 Proportional navigation guidance system.

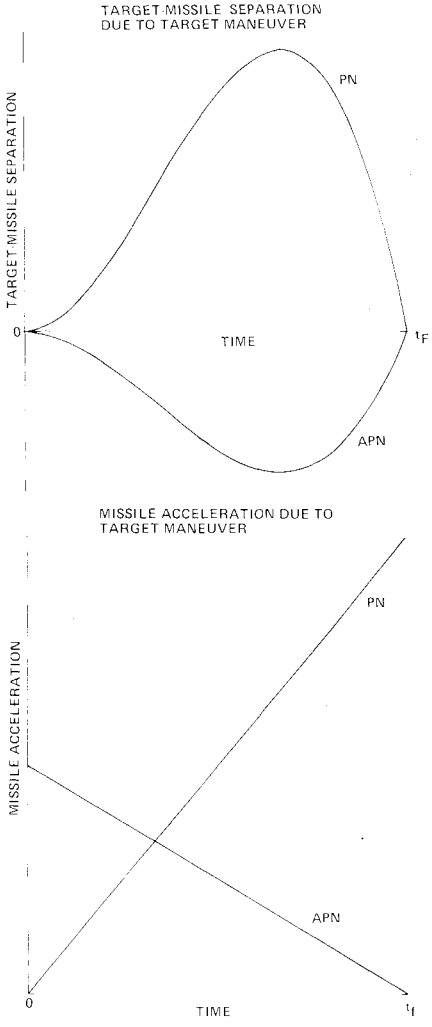

Fig. 5 Guidance method comparison.

The expression in the brackets of Eq. (2) represents the miss distance that would result (in the absence of target maneuver) if the missile made no further corrective accelerations and is referred to as the zero effort miss (ZEM). Therefore PN can be thought of as a guidance law in which acceleration commands are issued inversely proportional to the square of time-to-go and directly proportional to the ZEM. If target maneuver n_T is considered, the ZEM changes and a new guidance law known as augmented proportional navigation (APN) results

$$n_c = (N'/t_{go}^2)\,[y + \dot{y}t_{go} + \tfrac{1}{2}n_T t_{go}^2] \tag{3}$$

This guidance law is compared to PN, in terms of trajectory and acceleration histories, for the case of a maneuvering target with the results displayed in Fig. 5. Although both guidance laws achieve zero miss distance, the trajectory and acceleration histories are vastly different. The information concerning target maneuver enables APN guidance to use up less acceleration capability than PN while keeping it closer to an intercept course. In addition the APN acceleration history is monotonically decreasing unlike the monotonically increasing history of PN. It can be shown that for $N' = 3$ APN is optimal in the sense that it achieves zero miss distance utilizing the least integral square control effort.

Modern Guidance

In a modern guidance system, the ZEM is modified to take into account target maneuver and missile guidance system dynamics. If the guidance system dynamics can be represented by a first-order transfer function, with bandwidth ω, modern control theory[11] can be used to derive a guidance law which drives the miss distance to zero while minimizing the integral of the square of the acceleration:

$$y(t_F) = 0 \quad \text{subject to minimizing} \quad \int_0^{t_F} n_c^2 \mathrm{d}t$$

This law can be written as

$$n_c = \frac{N'}{t_{go}^2}\left[y + \dot{y}t_{go} + \tfrac{1}{2}n_T t_{go} - n_L \frac{(e^{-T} - 1 + T)}{\omega^2}\right] \tag{4}$$

where

$$T = \omega t_{go} \tag{5}$$

$$N' = \frac{6T^2\,(e^{-T} - 1 + T)}{2T^3 + 3 + 6T - 6T^2 - 12Te^{-T} - 3e^{-2T}} \tag{6}$$

The expression within the brackets of Eq. (4) is the ZEM and Eq. (6) shows that the effective navigation ratio is time-varying. Therefore this guidance law is a form of APN with an extra term to account for guidance system dynamics and a time-varying navigation ratio.

This guidance law, unlike PN, requires information concerning time-to-go t_{go}, guidance system bandwidth ω, and achieved missile acceleration n_L. Range measurements and additional filtering are required to estimate t_{go} and accelerometer measurements must now be fed into the guidance system. The states required for the implementation of this guidance law $(y, \dot{y}, n_T)$ can not be obtained from a simple low pass filter as was done with PN, but must be estimated.

A simple form of a Kalman estimator can be derived by considering the two most important stochastic disturbances in a guidance system, random target maneuver and glint noise. The resulting Kalman filter is stationary and represented by transfer function

$$\frac{\hat{y}}{y^*} = \frac{1 + 2s/\omega_0 + 2s^2/\omega_0^2}{1 + 2s/\omega_0 + 2s^2/\omega_0^2 + s^3/\omega_0^3} \tag{7}$$

with characteristic frequency ω_0 given by

$$\omega_0 = (\Phi_s/\Phi_N)^{1/6} \tag{8}$$

where Φ_s and Φ_N are estimates of the spectral density levels of the target maneuver process noise and glint measurement noise, respectively (see Appendices A and B for derivations via Wiener and Kalman filter formulations).[12-15] Thus the characteristic frequency of the filter increases with process noise and decreases with increasing measurement noise.

A typical implementation of a modern guidance system appears in Fig. 6. Here the line-of-sight angle is reconstructed from a seeker measurement of the boresight error and by integrating the rate gyro measurement of the seeker dish rate. This angle is then converted to relative target-missile position y^* by the multiplication of the range measurement. The signal

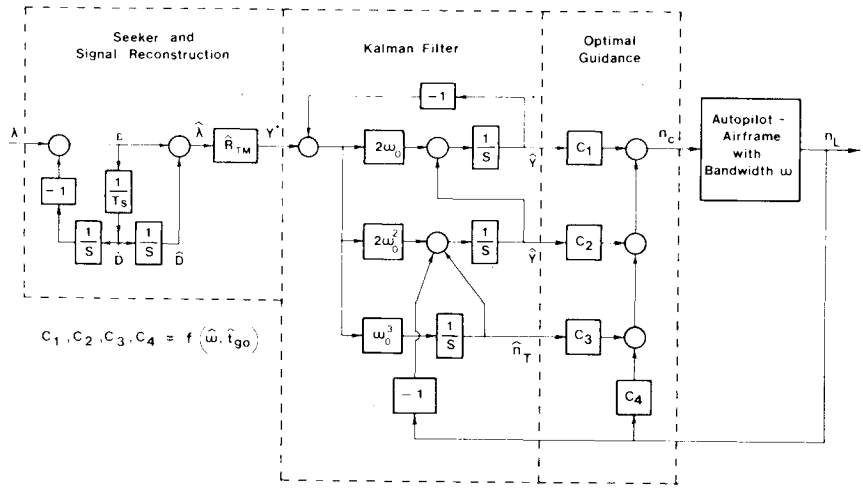

Fig. 6 Modern guidance system.

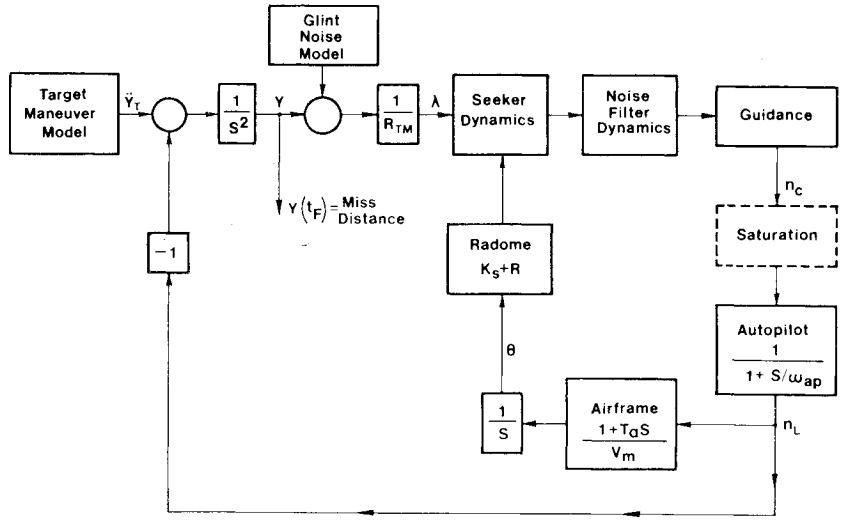

Fig. 7 Kinematic homing loop.

is then sent through the Kalman filter in order to obtain estimates of the necessary states for the implementation of the modern guidance law. These states are multiplied by control gains, which are functions of the estimated time-to-go and autopilot bandwidth, in order to generate an acceleration command. This command is applied to an acceleration autopilot in order to develop the command acceleration.

In summary the implementation of MGS requires some additional information that is not required by a classical PN guidance system. Estimates of range, measurement, and process noise statistics are needed for the implementation of the Kalman filter while estimates of time-to-go, guidance system bandwidth, and missile acceleration are needed for the implementation of the guidance law.

Performance Comparison

Both classical and modern guidance methods are now compared in terms of performance as measured by the rms miss distance. The comparison is made utilizing the linearized, but realistic model of the kinematic homing loop shown in Fig. 7. Here autopilot dynamics are represented by a first-order transfer function and only the two most important stochastic error sources are considered, namely glint noise and random target maneuver. The seeker, noise filter, and guidance dynamics have been previously represented in Figs. 4 and 6. In this case the Kalman filter of MGS is optimal since it is perfectly matched to the "real world" in that it has an exact dynamical model of the system along with perfect knowledge of the measurement and process noise statistics. With this methodology any deterioration in MGS performance will be caused solely by the guidance law.

Imbedded in the MGS guidance law is a dynamical model of the actual system. If this model is inaccurate or if the t_{go} estimate is lacking or inaccurate, MGS performance degrades. If the estimated time-to-go $\hat{t}_{go}$ is considered to be a simple function of t_{go} as shown in Eq. (9)

$$\hat{t}_{go} = At_{go} + B \tag{9}$$

then the influence of bias errors B and scale factor errors A on MGS system performance can be investigated. Typical miss distance results, shown in Fig. 8, indicate that errors in $\hat{t}_{go}$ result in rapid performance degradation of MGS. In fact, negative bias errors lead to guidance system instabilities of MGS. PN performance, superimposed on Fig. 8 is not sensitive to these errors. For this example PN achieves a miss of 4.3 ft. Therefore if the required miss distance was less than 4.3 ft, only MGS could meet that specification and then only if bias errors could be kept below 0.2 s and scale factor errors were between 0.68 and 1.35. If the required miss were greater than 4.3 ft, PN could meet the specification, but MGS could only meet the specification if bias and scale factor errors could be kept below the values of the curves in Fig. 8. Of course, PN does not use these quantities at all and therefore is not sensitive to such errors. In summary, the implementation of MGS places requirements not only on the algorithm for calculating t_{go}, but also on the special filtering needed to estimate range and range rate.

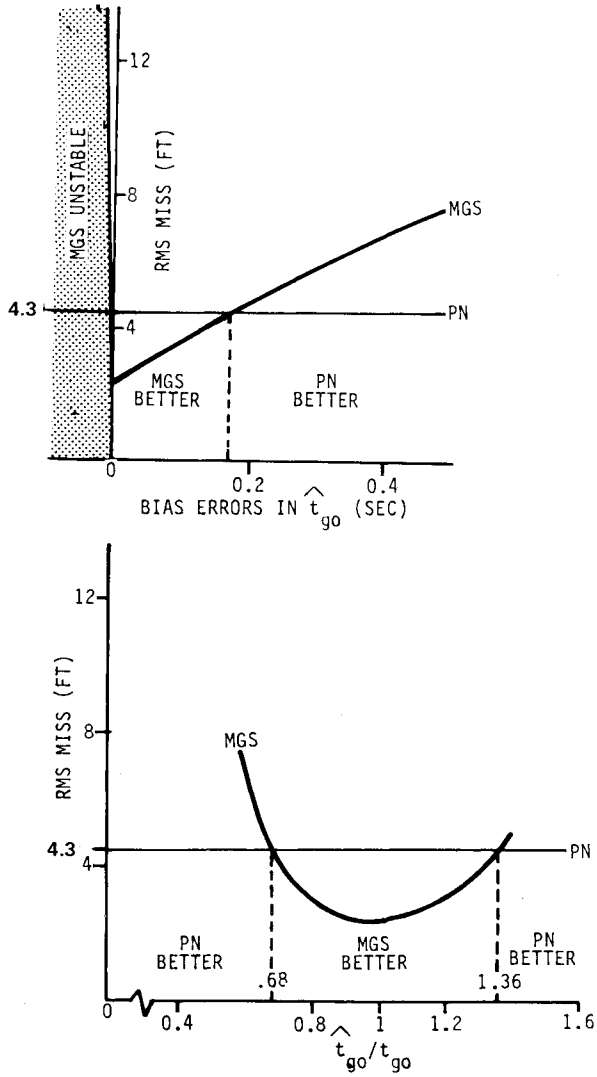

Fig. 8 Errors in estimating time to go seriously degrade MGS performance.

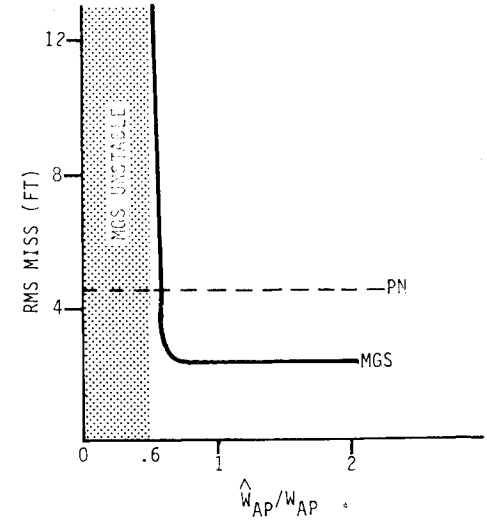

Fig. 9 Errors in estimating system dynamics can lead to MGS instability.

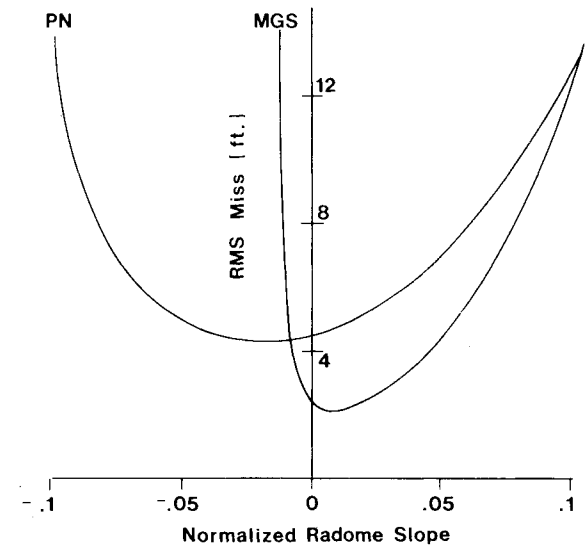

Fig. 10 Radome errors influence system performance.

Modern guidance system, unlike proportional navigation, attempts to compensate for autopilot dynamics by the use of a dynamic lead term in the missile acceleration command. In order to implement this concept, MGS requires an accurate measurement of the achieved missile acceleration and an estimate of the autopilot bandwidth W_{AP}. If this measurement is perfect and if the dynamic model within MGS is perfectly matched to the real world, optimum performance can be obtained. However, if for example, we assume that missile acceleration is measured perfectly, but the estimate of autopilot bandwidth is in error according to Eq. (10),

$$\hat{W}_{AP} = CW_{AP} \tag{10}$$

then the influence of scale factor errors C on MGS system performance can be investigated. Figure 9 shows that system instabilities result if the scale factor falls below 0.6. As before, PN performance is not sensitive to this error source. In this example, for miss distance below 4.3 ft, only MGS can meet the requirements if the scale factor is greater than 0.6. If the required miss distance is greater than 4.3 ft, PN can always meet the requirement, but MGS can only meet the specification if the scale factor is greater than 0.6. In summary, the implementation of MGS places requirements on allowable errors in dynamic modeling.

The nonhemispherical shape of the missile radome causes distortion of the incoming radar beam. As the radar beam passes through the radome a refraction effect takes place and the net result is an error in the angle of the apparent target. The radome error slope R is a measure of the distortion taking place and is a function of the gimbal angle, among other things.[6] The guidance system designer attempts to specify the manufacturing tolerances and the limits on the permissible variations of R. This error source is particularly important at high altitudes where the missile turning rate time constant T_α is large. This time constant in conjunction with large radome refraction slopes can cause guidance system instability. It is, therefore, of considerable practical importance to see how PN and MGS performance degrade in the presence of radome slope errors. Typical high-altitude performance results for both guidance systems are shown in Fig. 10. The results indicate that the PN guidance system has more of a tolerance to radome errors than does MGS. In this regard PN is more robust.

Figure 10 indicates that the MGS implementation is more sensitive to negative radome slopes than positive slopes. In a practical design, the seeker stabilization loop gain could be adjusted to bias the radome, thus insuring only positive slopes. It is for this reason that the allowable radome slope range is more of an important measure than the average radome slope. In fact, the allowable radome slope range is one important measure used in guidance system design to specify manufacturing tolerances on the radome. The average

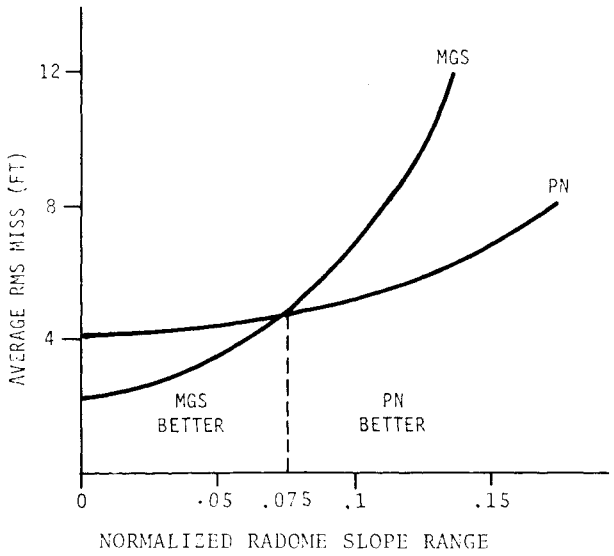

Fig. 11 PN allows greater flexibility in radome design.

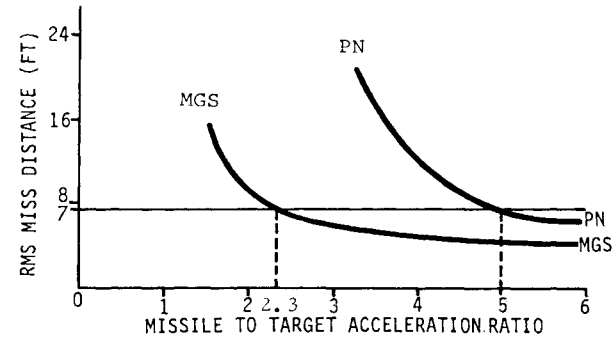

Fig. 12 MGS requires less acceleration due to target maneuver.

rms miss distance due to a radome slope range can be calculated from the information provided in Fig. 10. Typical results showing the sensitivity of both guidance systems to radome slope range is displayed in Fig. 11. This figure shows that when the radome is taken into consideration, MGS can only offer superior miss distance performance if the allowable radome slope range is less than 0.075. Otherwise PN yields smaller average rms miss distances. Nevertheless, if a radome slope range less than 0.075 can be met, MGS yields less miss distance.

Finally, missile acceleration saturation, one of the most important guidance system nonlinearities in the performance comparison, is considered. Since MGS predicts intercept using estimates of target acceleration and measurement of missile acceleration, it requires less acceleration than PN to hit a maneuvering target. In Fig. 12, where rms miss is plotted vs the missile-to-target acceleration ratio for both guidance system implementations, it is evident that PN requires a larger acceleration advantage over the target than MGS to achieve a specific miss distance. For example, to achieve an rms miss of less than 7 ft, PN requires a 5-to-1 acceleration advantage over the target whereas MGS requires only a 2.3-to-1 advantage. This reduced acceleration requirement extends the missile's zone of effectiveness against maneuvering targets and is the major advantage of MGS over PN.

Conclusion

A modern guidance system (MGS) and a proportional navigation (PN) guidance system designed to meet the same miss distance specification yield different implementation of subsystems, and each subsystem must meet a different set of requirements. A modern guidance system imposes more severe requirements on radome refraction slope and on knowledge of the system dynamics, but it does not require as much maximum missile normal acceleration to intercept an accelerating target. If the miss distance specification is extremely small, only MGS can do the job. Thus the additional instrumentation and subsystem requirements is the price that must be paid to meet severe miss distance requirements. If the miss distance specification is such that both MGS and PN can do the job, then instrumentation specifications can be relaxed in favor of more missile normal acceleration capability. When sufficient missile acceleration is available, PN offers the least stringent instrumentation requirements. Thus, if component tolerances can be met, MGS has the smallest miss distance, but as component tolerances or measurement errors degrade, the performance of MGS degrades faster than that of PN until, at relatively large component or measurement errors, PN has less miss distance than MGS.

Appendix A: Wiener Optimal Filter

The disturbances entering the guidance system are considered to be white glint noise with spectral density Φ_N and random target maneuver. In this paper the maneuver is considered to be a step function whose initiation time is uniformly distributed over the flight time. It can be shown[12] that integrated white noise has the same autocorrelation function as this maneuver process. The optimal filter with transfer function H_0 can be derived by either Wiener or Kalman filter theory.

The Wiener filter formulation is based upon the diagram of Fig. A1. The problem is to find H_0 which will minimize the integral of the mean square signal

$$\left[\text{minimize } \int_0^\infty e^2 dt\right]$$

The optimal transfer function H_0 can be found from the explicit solution of the Wiener-Hopf integral equation

$$H_0 = \frac{1}{(W_S + W_N)^+}\left[\frac{W_S}{(W_S + W_N)^-}\right]_+ \tag{A1}$$

where W_S and W_N are the spectral densities of the signal and noise, $(W_S + W_N)^+$ represents that part which has all its poles and zeroes in the left half-plane, and $(W_S + W_N)^-$ that part which has all its poles and zeroes in the right half-plane. The expression $[\cdot]_+$ is the component of $[\cdot]$ which has all its poles in the left half-plane. In order to obtain $[\cdot]_+$ we expand $[\cdot]$ in partial fractions and throw away all the terms corresponding to poles in the right half-plane. From Fig. A1 the output spectral densities of the signal and noise, W_S and W_N, can be expressed in terms of the input spectral densities, Φ_S and Φ_N, and the shaping network transfer function as

$$W_S = \Phi_S / -S^6 \tag{A2}$$

$$W_N = \Phi_N \tag{A3}$$

Therefore

$$W_S + W_N = \frac{\Phi_S}{-S^6} + \Phi_N = \frac{\Phi_S(1 - \Phi_N S^6/\Phi_S)}{-S^6} \tag{A4}$$

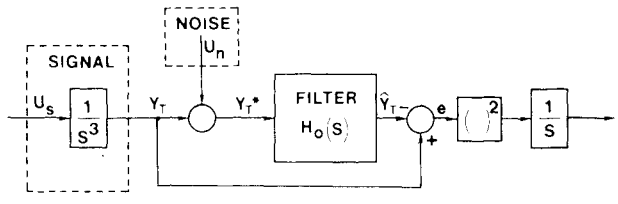

Fig. A1 Wiener filter formulation.

If we define

$$\omega_0 = (\Phi_S/\Phi_N)^{1/6} \tag{A5}$$

then Eq. (A4) can be factored

$$W_S + W_N = \frac{\Phi_S(1 - S^6/\omega_0^6)}{-S^6}$$

$$= \Phi_S \frac{(1 + 2S/\omega_0 + 2S^2/\omega_0^2 + S^3/\omega_0^3)}{(S^3)} \frac{(1 - 2S/\omega_0 + 2S^2/\omega_0^2 - S^3/\omega_0^3)}{(-S^3)} \tag{A6}$$

Therefore

$$(W_S + W_N)^+ = \Phi_S \frac{(1 + 2S/\omega_0 + 2S^2/\omega_0^2 + S^3/\omega_0^3)}{(S^3)} \tag{A7}$$

$$(W_S + W_N)^- = \frac{(1 - 2S/\omega_0 + 2S^2/\omega_0^2 - S^3/\omega_0^3)}{(-S^3)} \tag{A8}$$

Substitution of Eqs. (A2), (A7) and (A8) into (A1) yields

$$H_0 = \frac{S^3}{\Phi_S(1 + 2S/\omega_0 + 2S^2/\omega_0^2 + S^3/\omega_0^3)} \times \left[\frac{\Phi_S}{S^3(1 - 2S/\omega_0 + 2S^2/\omega_0^2 - S^3/\omega_0^3)}\right]_+ \tag{A9}$$

The expression in the brackets of Eq. (A9) can be expanded by partial fractions yielding

$$[\cdot]_+ = \left[\Phi_S\left(\frac{1}{S^3} + \frac{2/\omega_0}{S^2} + \frac{2/\omega_0^2}{S} + \frac{1/\omega_0^3}{1 - S/\omega_0} - \frac{1/\omega_0 + S}{1 - S/\omega_0 + S^2/\omega_0^2}\right)\right]_+ \tag{A10}$$

Eliminating those terms with poles in the right half-plane leaves

$$[\cdot]_+ = \Phi_S\left(\frac{1}{S^3} + \frac{2/\omega_0}{S^2} + \frac{2/\omega_0^2}{S}\right) \tag{A11}$$

which simplifies to

$$[\cdot]_+ = \Phi_S\left(\frac{1 + 2S/\omega_0 + 2S^2/\omega_0^2}{S^3}\right) \tag{A12}$$

Substitution of Eq. (A12) into (A9) yields the optimal transfer function

$$H_0 = \frac{1 + 2S/\omega_0 + 2S^2/\omega_0^2}{1 + 2S/\omega_0 + 2S^2/\omega_0^2 + S^3/\omega_0^3} \tag{A13}$$

Appendix B: Kalman Optimal Filter

The same transfer function can also be obtained by the Kalman formulation.

The state and measurement equations can be derived from the plant, shown in Fig. B1, and are

$$\begin{bmatrix} \dot{y}_T \\ \ddot{y}_T \\ \dddot{y}_T \end{bmatrix} = \begin{bmatrix} 0 & 1 & 0 \\ 0 & 0 & 1 \\ 0 & 0 & 0 \end{bmatrix} \cdot \begin{bmatrix} y_T \\ \dot{y}_T \\ \ddot{y}_T \end{bmatrix} + \begin{bmatrix} 0 \\ 0 \\ u_S \end{bmatrix} \tag{B1}$$

$$\underline{\dot{X}} = \underline{F} \cdot \underline{X} + \underline{U}$$

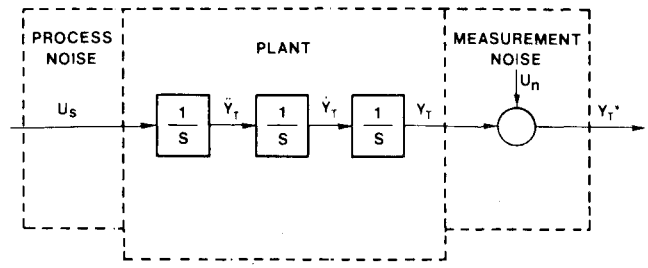

Fig. B1 Kalman filter formulation.

$$Y_T^* = [1\ 0\ 0] \cdot \begin{bmatrix} y_T \\ \dot{y}_T \\ \ddot{y}_T \end{bmatrix} + u_N \tag{B2}$$

$$\underline{z} = \underline{H} \cdot \underline{X} + V$$

The Kalman filter equation is

$$\dot{\underline{\hat{X}}} = \underline{F} \cdot \underline{\hat{X}} + \underline{K}[\underline{z} - \underline{H}\underline{\hat{X}}] \tag{B3}$$

where the Kalman gains $\underline{K}$ are determined from the following matrix Riccati equations:

$$\dot{\underline{P}} = \underline{F}\underline{P} + \underline{P}\underline{F}^T - \underline{P}\underline{H}^T\underline{R}^{-1}\underline{H}\underline{P} + \underline{Q} \tag{B4}$$

$$\underline{K} = \underline{P}\underline{H}^T\underline{R}^{-1} \tag{B5}$$

where

$$Q = \begin{bmatrix} 0 & 0 & 0 \\ 0 & 0 & 0 \\ 0 & 0 & \Phi_s \end{bmatrix} \quad \text{and} \quad \underline{R} = \Phi_N \tag{B6}$$

Recognizing that the covariance matrix $\underline{P}$ is symmetric, the scalar equations representing the steady-state solution ($\dot{\underline{P}} = \underline{0}$) can be written from Eq. (B4) as

$$P_{11}^2 = 2P_{12}\Phi_N \qquad P_{12}^2 = 2P_{23}\Phi_N \qquad P_{13}^2 = \Phi_S\Phi_N$$

$$P_{11}P_{12} = \Phi_N(P_{22} + P_{13}) \qquad P_{11}P_{13} = P_{23}\Phi_N \qquad P_{12}P_{13} = P_{33}\Phi_N \tag{B7}$$

After some algebra, the solutions to Eq. (B7) can be substituted into Eq. (B5) yielding the steady state Kalman gains

$$\underline{K} = \begin{bmatrix} K_1 \\ K_2 \\ K_3 \end{bmatrix} = \begin{bmatrix} 2(\Phi_S/\Phi_N)^{1/6} \\ 2(\Phi_S/\Phi_N)^{1/3} \\ (\Phi_S/\Phi_N)^{1/2} \end{bmatrix} \tag{B8}$$

Defining

$$\omega_0 = (\Phi_S/\Phi_N)^{1/6} \tag{B9}$$

the gain matrix becomes

$$\underline{K} = \begin{bmatrix} 2\omega_0 \\ 2\omega_0^2 \\ \omega_0^3 \end{bmatrix} \tag{B10}$$

The filter equations are obtained by substituting Eq. (B10) into Eq. (B3) yielding

$$\begin{bmatrix} \dot{\hat{y}}_T \\ \ddot{\hat{y}}_T \\ \dddot{\hat{y}}_T \end{bmatrix} = \begin{bmatrix} 0 & 1 & 0 \\ 0 & 0 & 1 \\ 0 & 0 & 0 \end{bmatrix} \begin{bmatrix} \hat{y}_T \\ \dot{\hat{y}}_T \\ \ddot{\hat{y}}_T \end{bmatrix} + \begin{bmatrix} 2\omega_0 \\ 2\omega_0^2 \\ \omega_0^3 \end{bmatrix} \cdot [y_T^* - \hat{y}_T] \tag{B11}$$

The transfer function between the position estimate output and the position measurement input easily can be obtained from Eq. (B11) as

$$\frac{\hat{y}_T}{y_T^*} = \frac{1 + 2S/\omega_0 + 2S^2/\omega_0^2}{1 + 2S/\omega_0 + 2S^2/\omega_0^2 + S^3/\omega_0^3} \tag{B12}$$

This is identical to the transfer function obtained by the Wiener filter approach.

References

[1] Bryson, A.E. and Ho, Y.C., *Applied Optimal Control,* Blaisdell Publishing Company, Waltham, Mass., 1969, pp. 424-426.

[2] Willems, G., "Optimal Controllers for Homing Missiles," U.S. Army Missile Command, Redstone Arsenal, Ala., Rept. RE-TR-68-15, Sept. 1968.

[3] Willems, G., "Optimal Controllers for Homing Missiles with Two Time Constants," U.S. Army Missile Command, Redstone Arsenal, Ala., Rept. RE-TR-69-20, Oct. 1969.

[4] Price, C.F., "Optimal Stochastic Guidance Laws for Tactical Missiles," The Analytical Sciences Corporation, Reading, Mass., Rept. TR-170-2, Sept. 1971.

[5] Phillips, T.L., "Anti-Aircraft Missile Guidance," *Electronic Progress,* Raytheon Co., March-April 1958, pp. 1-5.

[6] Nesline, F.W., "Missile Guidance for Altitude Air Defense," *Journal of Guidance and Control,* Vol. 2, July-Aug. 1979, pp. 283-289.

[7] Benecke, T. and Quick, A.W. (eds.), "History of German Guided Missiles Development," AGARD First Guided Missiles Seminar, Munich, Germany, April 1956.

[8] Yuan, C.L., "Homing and Navigational Courses of Automatic Target-Seeking Devices," RCA Laboratories, Princeton, N.J., Rept. PTR-12C, Dec. 1943.

[9] Bennett, R.R. and Mathews, W.E., "Analytical Determination of Miss Distances for Linear Homing Navigation Systems," Hughes Aircraft Co., Culver City, Calif., Tech. Memo. 260, March 1952.

[10] Yuan, C.L., "Homing and Navigational Courses of Automatic Target-Seeking Devices," *Journal of Applied Physics,* Vol. 19, Dec. 1948, pp. 1122-1128.

[11] Cottrell, R.G., "Optimal Intercept Guidance for Short-Range Tactical Missiles," *AIAA Journal,* Vol. 9, July 1971, pp. 1414-1415.

[12] Fitzgerald, R.J. and Zarchan, P., "Shaping Filters for Randomly Initiated Target Maneuvers," *Proceedings of AIAA Guidance and Control Conference,* Palo Alto, Calif., Aug. 1978, pp. 424-430.

[13] Wiener, N., *Extrapolation, Interpolation and Smoothing of Stationary Time Series,* MIT Press, Cambridge, Mass., 1949, pp. 81-103.

[14] Newton, G.C., Gould, L.A., and Kaiser, J.F., *Analytical Design of Linear Feedback Controls,* John Wiley and Sons, Inc., New York, 1957, pp. 140-159.

[15] Kalman, R.E. and Bucy, R., "New Results in Linear Filtering and Prediction," *Journal of Basic Engineering (ASME),* Vol. 83D, 1961, pp. 95-108.